International Journal of Nanomedicine Dovepress

Open Access Full Text Article ORIGINAL RESEARCH

A Novel pH-Responsive Nano-Sized Lanthanum-Doped Polyvinyl Alcohol-Carbon Quantum Dot Composite for Root Canal Irrigation

Lihua Yu[1,2,*], Chunxia Zhang[3,*], Jie Yang[4], Lu Li[3]

[1]Department of Pediatric Dentistry, Tianjin Stomatological Hospital, School of Medicine, Nankai University, Tianjin, 300041, People's Republic of China; [2]Tianjin Key Laboratory of Oral and Maxillofacial Function Reconstruction, Tianjin, 300041, People's Republic of China; [3]Tianjin Baogang Rare Earth Research Institute Co., Ltd, Tianjin, 300300, People's Republic of China; [4]Department of Stomatology, The Second Hospital of Tianjin Medical University, Tianjin, 300211, People's Republic of China

*These authors contributed equally to this work

Correspondence: Chunxia Zhang, Tianjin Baogang Rare Earth Research Institute Co., Ltd, Block B, Building 5, No. 6, Huafeng Street, Huaming High-Tech Industrial Zone, Dongli District, Tianjin, 300300, People's Republic of China, Tel +86-022-58910562, Email zcx19941002@163.com

Purpose: The primary goals of endodontic therapy are to eliminate microbes and prevent reinfection. Persistent root canal infections and failure of root canal therapy are primarily attributed to the presence of bacteria, particularly E. faecalis. Chemical irrigants play a crucial role in complementing mechanical instrumentation in ensuring adequate disinfection. However, current techniques and available irrigants are limited in their ability to achieve optimal sterilization of the root canal system. In this study, we developed a novel material called La@PCDs by combining CQD-PVA and lanthanum for root canal irrigation.

Methods: A one-pot hydrothermal method was used to prepare composites of lanthanum and CQD-PVA (La@PCDs). Scanning electron microscopy (SEM), Fourier-transform infrared (FTIR) spectroscopy and the particle size were employed to characterize La@PCDs. ROS generation was evaluated by measuring the fluorescence intensity emitted at 525 nm from 2′,7′-dichlorodihydro-fluorescein diacetate (DCFH-DA). In vitro experiments were conducted to assess the effectiveness of the nanoparticles in combating Enterococcus faecalis and eradicating in situ biofilm eradication in root canal. Furthermore, cytotoxicity assessments were carried out to demonstrate the safety of La@PCDs.

Results: SEM and FTIR results showed that La@PCDs were successfully prepared and exhibiting a homogeneous size distribution and irregular morphology. ROS assessment demonstrated that La@PCDs have a synergistic effect, promoting the production of a large number of ROS. This effect only occurred under acidic PH conditions. The inherent acidity in the biofilm microenvironment can act as internal stimulus. In vitro experiments revealed superior antibacterial efficiency under acidic conditions without causing significant cytotoxicity compared to the commonly used NaClO irrigant. The biosafety of La@PCDs was confirmed.

Conclusion: Compared to existing materials, these nanoparticles exhibit favorable antibacterial and anti-biofilm properties, along with improved biocompatibility. These findings emphasize the potential of the integrated La@PCDs as a promising option for enhancing root canal irrigation and disinfection.

Keywords: lanthanum, La, reactive oxygen species, ROS, pH-response, antimicrobial, root canal irrigation

Introduction

The primary causative factors of pulpitis and apical periodontitis (AP) are widely recognized as bacteria and the substances they produce.[1] Microbial communities can form biofilm structures that firmly attach to dentin in the root canal system.[2] Therefore, effective chemomechanical debridement is crucial for eliminating root canal infections. Biofilm bacteria derive advantages from multiple factors that contribute to their survival, one of which is the presence of a self-generated extracellular polymeric substances (EPS) matrix. This matrix serves as a protective barrier against root canal disinfectants and reduces their effectiveness.[3] Additionally, anatomically small regions of the root canal system are difficult to adequately clean, leading to

Received: 28 April 2024
Accepted: 28 September 2024
Published: 6 November 2024

residual infection.[4] Furthermore, irrigants often fail to reach deep into the dentinal tubules, allowing bacteria, such as Enterococcus faecalis (E. faecalis), typically associated with post-treatment ineffectiveness, to survive. The prolonged survival of E. faecalis within root canals is attributed to its ability to withstand highly alkaline and nutrient-deprived environments, whilst facilitating biofilm formation.[5,6] Moreover, it can penetrate deep into dentin tubules, effectively evading phagocytosis by host cells.[7] The importance of irrigating agents cannot be overstated in terms of the eradication and prevention of root canal infections.

Sodium hypochlorite (NaOCl) is widely utilized as an irrigating solution in endodontics, with concentrations ranging from 0.5% to 5.25%.[8] It is highly regarded for its capacity to dissolve tissues and combat microorganisms; however, improper usage can lead to detrimental effects such as dentin weakening and periapical tissue damage.[9] Ethylenediaminetetraacetic acid (EDTA), another chelating agent frequently used for smear layer removal, has limited effectiveness as an irrigant owing to its weak antimicrobial properties.[10] Consequently, there has been an increasing focus on nanoparticle-based irrigation that demonstrate the potential to eradicate root canal biofilms. Some silver nanoparticles and stimuli-responsive nanoagents have been developed for this purpose.[11,12]

Rare earth elements, commonly known as "industrial vitamins", are a vital resource with extensive applications in various industries, including in agriculture and medical materials. The investigation into the antimicrobial properties of rare earth elements has been ongoing since the early 20th century.[13] Lanthanum (La) and its compounds have attracted significant interest due to their exceptional characteristics, such as low toxicity, spectral characteristics, and efficacy as antibiotics at low doses.[14] La^{3+} interacts with key components on the surface of bacterial cell membranes (such as peptidoglycans, phospholipids, and proteins) to form stable complexes that alter membrane permeability. This internal accumulation enables La^{3+} to bind to DNA and proteins within bacterial cells, thereby disrupting the metabolism and inhibiting bacterial growth.[15] In addition, rare earth elements can generate reactive oxygen species through electron transitions during photocatalysis. However, certain limitations such as poor mechanical properties, low thermal stability, and hormetic effects on microbes have hindered their widespread application.[16] The unpaired electrons present in the 4f subshell of rare-earth elements facilitate active coordination with the outer electrons from other elements, resulting in the synthesis of antibacterial rare-earth complexes.[17] Consequently, the doping of nanomaterials with rare-earth elements to create multifunctional nanomaterials has become an area of significant research interest.

Carbon quantum dots (CQDs) are nanomaterials that are typically smaller than 10 nm in size and possess favorable fluorescence characteristics. CQDs exhibit exceptional biocompatibility, high water solubility, stable fluorescence properties, and high fluorescence intensity properties. Importantly, CQD surfaces contain numerous hydroxyl, carboxyl, and epoxy functional groups that can be modified to create versatile nanomaterials.[18] Polyvinyl alcohol (PVA) is a biocompatible water-soluble polymer that benefits from advanced synthetic techniques, and facile processing and shaping methods. It has applications in biomedical dressings, light-conversion materials, and shape-memory materials.[19] Recently, researchers have successfully synthesized novel functional composites by combining CQD with PVA polymers. Kumar et al conducted a study where nitrogen-doped CQDs were incorporated into PVA to precisely tune the refractive index of the resulting CQD-PVA composite from approximately 1.55 to 1.90 at a wavelength of 700nm.[20] The combination of low-energy states in CQDs and insulating PVA, as demonstrated by Ambasankar et al, encouraged efficient charge trapping capabilities in these composites.[21] Therefore, incorporating quantum dots (QDs) into a polymer matrix is a convenient strategy for protecting them from their surrounding environment, and for exploring the unique properties of the resulting composites.

In this study, a one-pot hydrothermal method was used to prepare lanthanum and CQD-PVA composites (La@PCDs). The antimicrobial properties of lanthanum have also been identified. However, the composite effect when lanthanum is combined with CQD-PVA is unknown. We investigated the material characteristics of La@PCDs, including the particle size and FTIR spectra. This included the generation of ROS at different pH levels to explore their potential as pH-responsive nanofunctional materials. In addition, the efficacy of this material in eliminating bacteria and eradicating biofilms was evaluated for its potential application in the treatment of endodontic infections.

Materials and Methods

Materials

Lanthanum chloride ($LaCl_3$), $La(NO_3)_3{\cdot}6H_2O$ and PVA (MW 1750) were purchased from Merck Chemical Technology Co., Ltd (Shanghai, China). Luria-Bertani (LB) medium and brain heart infusion (BHI) were purchased from Beijing Land Bridge Technology Co., Ltd (Beijing, China). Cell Counting Kit-8 and SYTO 9/PI Live/Dead Bacterial Double Stain Kit were purchased from BestBio (Shanghai, China). Rhodamine–phalloidin and 4'6-diamidino-2-phenyl-indole (DAPI) were purchased from Solarbio Co., Ltd (Beijing, China).

Preparation of La@PCDs

La@PCDs was prepared according to a hydrothermal method reported before[1]. In brief, Approximately 80 mL of deionized water was added to a 200 mL beaker. 35 grams of $La(NO_3)_3{\cdot}6H_2O$ was then added, and the mixture was then vigorously stirred. 5 g of PVA was weighed, added to the blended solution, and uniformly mixed on a magnetic stirrer for 10 min. Afterwards, the mixture was transferred into a hydrothermal reactor lined with polytetrafluoroethylene, and the reaction was initiated at an elevated temperature of 180°C within an oven for a period spanning over 6 hours. The resultant product was then subjected to drying and concentration before being transferred to a Muffle furnace where it underwent calcination at a high temperature of 1200°C for a duration of 3 hours in order to obtain La@PCDs.

Characterization

Scanning electron microscopy (SEM) was performed using an Hitachi Regulus 8100 SEM (Hitachi Limited, JP). Fourier-transform infrared (FTIR) spectroscopy was performed using a Nicolet iS 10 FTIR spectrometer (Thermo Fisher Scientific, USA). The particle size was determined on the Malvern Zetasizer Nano ZS90 nanometer particle size and Zeta Potential analyzer (DLS) (Malvern Instruments Limited, UK). X-ray photoelectron spectroscopy (XPS, Thermo Scientific K-Alpha, USA), the fluorescence and quantum yield (QY, Edinburgh FLS1000) were performed to characterize the materials.

Determination of ROS Generation

Determining the amount of ROS generation by the different materials was completed by measuring the fluorescence intensity at 525 nm emitted from 2′,7′-dichlorodihydrofluorescein diacetate (DCFH-DA). Specifically, 0.1 mg of LaNPs and La@PCDs were placed in tubes containing 1 mL of deionized water, followed by the addition of 20 mL of DCFH-DA. The fluorescence intensity was measured using a spectrofluorophotometer (RF-5301PC, Shimadzu) at an excitation wavelength of 488 nm.

Assessment of Antimicrobial Activity in vitro

Minimum Inhibitory Concentration and Minimum Microbicidal Concentrations of La@PCDs and LaNPs

The determination of minimal inhibitory concentration (MIC) and minimal bactericidal concentration (MBC) was conducted through a modified technique involving microdilution in broth. In brief, bacterial suspension of E. faecalis was cultured to the mid-exponential phase and diluted to 2×10^5 CFU mL^{-1}. 1. Subsequently, a mixture of 100 μL of diluted bacterial suspension and 100 μL of various concentrations of LaNPs and La@PCDs was added to a sterile flat-bottom plate, resulting in a total volume of 200 μL. This yielded an appropriate final concentration of suspension (10^5 CFU mL^{-1}), with the LaNPs and La@PCDs at gradient concentrations ranging from 64 to 0.03 mg mL^{-1}. The plates were incubated for a duration of 18 hours at a temperature of 37 °C. The optical density (OD) values were measured per hour at a wavelength of 600 nm (OD_{600}). The MIC was determined as the lowest concentration of LaNPs and La@PCDs that preserved the initial optical density (OD). The determination of MBC was conducted utilizing the agar plate dilution technique. Culturing 100 μL aliquots extracted from microwells on agar plates for a duration of 48 hours and the lowest concentration at which no colonies were observed was defined as MBC. All experiments were repeated three times.

Antimicrobial Activity in vitro Compared to NaCLO

First, 2 mL of three different solutions including LaNPs, La@PCDs and NaClO were prepared and added 20 μL of diluted E. faecalis bacterial suspension. Then, the sample solutions containing bacteria were added 1000 times saline solution to terminate sterilization when the reaction time was 0,30,60,90,120,150,180 seconds respectively. The bacterial activity was recorded by CCK8 method and the kinetic curve of bacterial growth was drawn.

The effectiveness of the nanoparticles in inhibiting the growth of E. faecalis (ATCC 29212) was evaluated using a method involving successive dilutions. Specifically, the initial tube containing 1 mL of deionized water was supplemented with 1 mg of LaNPs or La@PCDs. The negative control consisted of H_2O, whereas the positive control contained 5% NaClO. After thorough mixing, the solution (0.5 mL) obtained from the last tube was sequentially removed to the next tube along with deionized water (0.5 mL) to reduce its concentration by 50%. E. faecalis strains of the mid-exponential phase were harvested and diluted to a concentration of 10^6 CFU mL^{-1}. 0.5 mL diluted bacterial suspension was introduced into the serially diluted solutions, followed by irradiation with or without ultrasound waves at a frequency of 1.0 MHz and an intensity of 0.5 W cm^{-2} for a period of 3 min. Afterwards, a 100 mL sample was diluted and evenly distributed onto agar plates containing LB or BHI medium. The plates were then incubated at approximately 37°C for up to 24 hours, during which time the number of colony forming units (CFUs) on each agar plate was counted. This was used as an indicator for assessing antimicrobial effectiveness. The treated mixture was diluted using the BHI medium and added to 96-well plate. The plate was then positioned in an incubator set at approximately 37°C. After a designated incubation period of either 12 or 24 h, the absorbance of junye was measured by Elisa. Each subgroup was comprised of three independent samples, and all experiments were repeated three times.

Biofilm Eradication Effect in vitro

To evaluate the efficacy of the nanoparticles in eradicating biofilms under laboratory conditions, laser scanning confocal microscopy (CLSM) (Carl Zeiss Microscopy, Oberkochen, Germany) was used to visualize the biofilms. Initially, a prepared suspension containing E. faecalis bacteria was placed in a confocal dish and statically cultured at 37°C for 48 h to facilitate mature biofilm formation on the dish surface. Subsequently, the media were removed, and the biofilms were rinsed thrice with sterile PBS to separate free-floating bacteria. Next, 1 mL of PBS (control group), LaNPs, 5% NaCLO, or the synthesized La@PCDs were added to the biofilm and incubated for 3 min. The treated biofilms were rinsed by PBS and stained using the Live/Dead BacLight Bacterial Viability Kit (BestBio Co., Shanghai, China). The viability of E. faecalis cells within the biofilm (live/dead) was observed using CLSM by analyzing the relative green or red fluorescence signals using an imaging software (Zeiss Zen lite, Oberkochen, Germany). Each experimental group consisted of three independent samples, and measurements were performed in triplicate.

Assessment of Biofilm Removal in Root Canal System

The fresh extraction of premolars were collected from human subjects specifically for orthodontic purposes and the patients provided informed consent in accordance with the Declaration of Helsinki. The Human Assurance Committee of Tianjin Medical University approved the research protocol used in this study. The tooth crown was removed to obtain the root segment according to a method similar to the study by Ye's study.[22] A total of 60 teeth exhibiting single root canal morphology were involved in the investigation. For the purpose of root canal shaping, stainless-steel K-files and ProTaper Gold nickel-titanium rotary instruments were employed up to F3 size. Following the use of each instrument, irrigation with 2 mL of 5% NaOCl solution was performed. One single trained researcher performed the entire root canal preparation process. To neutralize any remaining intracanal NaOCl, 2 mL of 5% sodium thiosulfate was used. Subsequently, the inoculum suspension of E. faecalis was obtained by adjusting the optical density (OD) of a mid-exponential suspension to 0.5 at a wavelength of 600 nm. The sterilized root segments were immersed in a suspension containing an inoculum of E. faecalis. All samples were incubated at a temperature of 37 °C and the culture medium was exchanged every 48 hours to facilitate the growth of biofilm within the root canal system. Four weeks later, the root segments were rinsed with four solutions: (1) PBS as a negative control, (2) LaNPs, (3) La@PCDs, and (4) 5% NaClO irrigant as a positive control. Each root segment was submerged in a tube containing 2 mL of the respective solution for

a total duration of three minutes. Subsequently, rinsing with PBS took place before each specimen was longitudinally split in half. Finally, SEM analysis was conducted to examine the morphology of E. faecalis biofilm in root canal surface.

Cytotoxicity Evaluation

The L929 mouse fibroblast cell line (obtained from the Cell Culture Center, Peking Union Medical College, China) was cultured in culture flask containing DMEM, 10% FBS and 1% PS at 37 °C in 5% CO_2. The culture medium was refreshed every two days, and the cells were performed every four days to ensure optimal growth conditions.

The cells were incubated in a 96-well plate at a density of 2000 cells per cm^2 at 37 °C in 5% CO_2. After 24 h, the culture medium was replaced with sterilized PBS (control), LaNPs, La@PCD, or diluted with 5% NaClO (1/10 ratio). The plate was further incubated for 4h before conducting the CCK-8 assay following the manufacturer's instructions. Each group contained three independent samples, and cytotoxicity measurements were performed in triplicate.

The cytotoxic effects of these substances were assessed by examining the cellular morphologies. The cell slides were placed in a 24-well plate and L929 cells were seeded at a density of 10^4 cells per cm^2. After incubation for 24 h, the culture medium was replaced with sterile PBS (control), LaNPs, La@PCDs, or a diluted solution of 5% NaClO. After 4 hours incubation period, the culture medium was aspirated and the cells were stained with rhodamine-phalloidin and DAPI following the manufacturer's guidelines. The morphology of cells was observed by a fluorescence microscope (Zeiss, Oberkochen, Germany).

Statistical Analysis

The data is presented as mean ± standard deviation, and each experiment was repeated three or more times. Statistical analyses were conducted using analysis of variance (ANOVA), with statistical significance defined as $p < 0.05$.

Results and Discussion

Characterization of La@PCDs

A novel La@PCDs base was prepared on the rare earth element La and a CQD-PVA composite via one-pot hydrothermal method (Figure 1). According to the SEM results, the La@PCDs were well-dispersed and exhibited a homogeneous size distribution and irregular morphology (Figure 2A). The particle size of the La@PCDs material measured approximately 697 nm, indicating its suitability for application in root canal therapy lotions due to its small dimensions (Figures 2D and S1). The content and valence states of La@PCD were determined by XPS (Figure 2B). La 3d spectra were presented in two peaks which centered at 852.82eV correspond to La $3d_{2/3}$, and other peaks located at 836.14eV are assigned to La $3d_{2/5}$. The

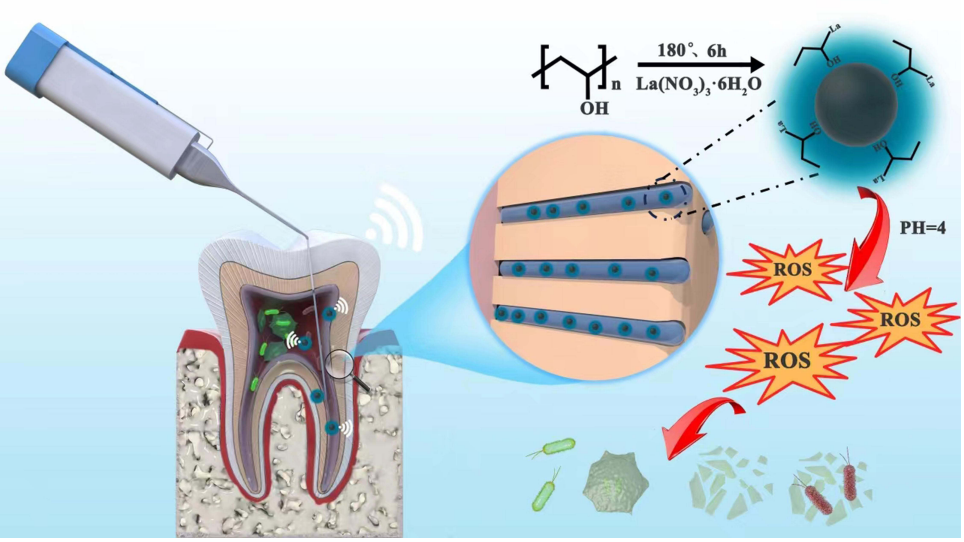

Figure 1 Schematic illustration of the formation of La@PCDs and bacteria-killing processes.

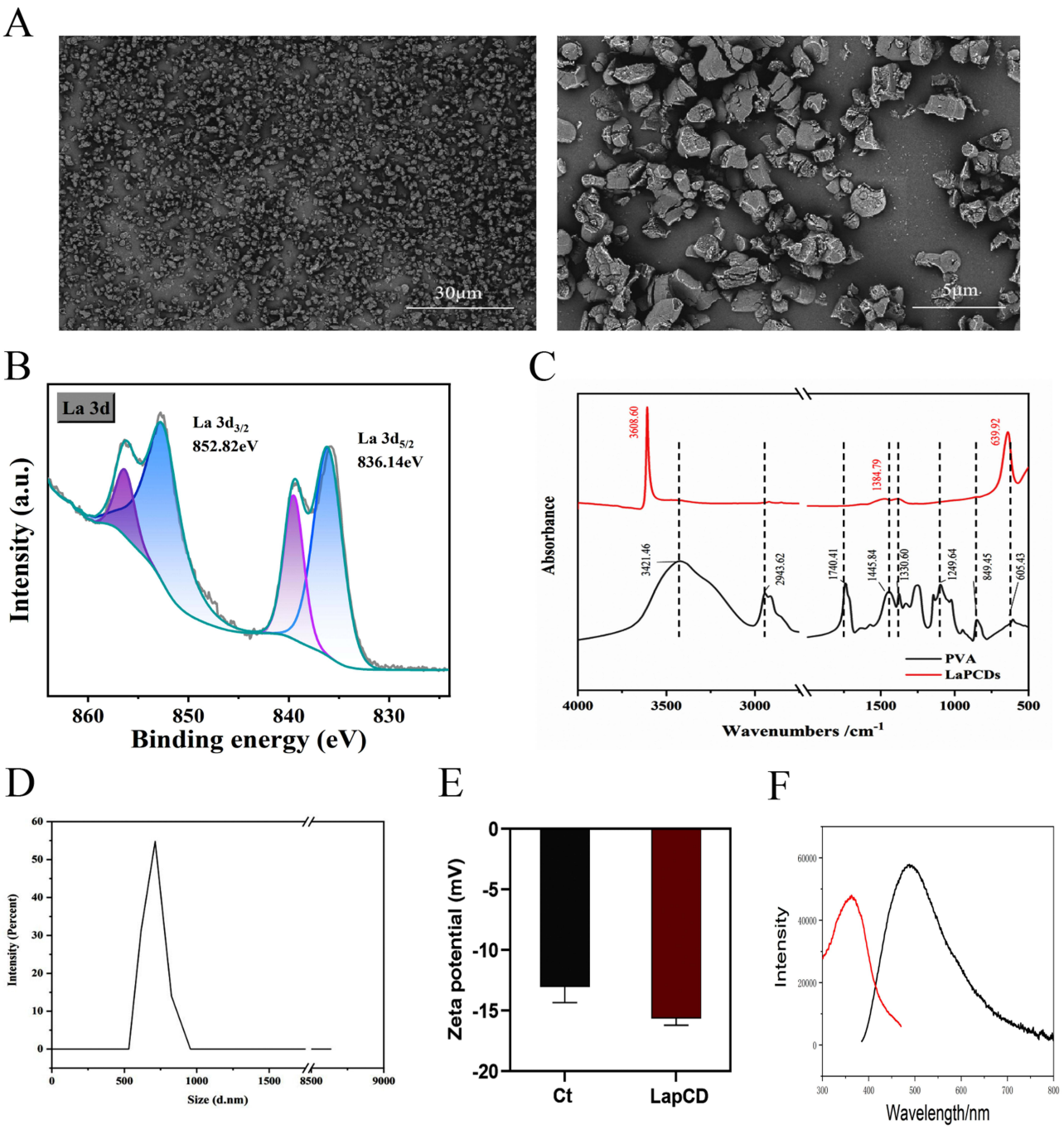

Figure 2 Characterization of La@PCDs: (**A**) SEM of La@PCDs (**B**) XPS of La@PCDs (**C**) FTIR spectra of PVA and La@PCDs. (**D**) Size of La@PCDs (**E**) Zeta potential (**F**) The fluorescence detection of La@PCDs.

energy difference between La $3d_{5/2}$ and La $3d_{3/2}$ states are nearly 16.68 eV, which is well in line with the character values of lanthanum in La@PCDs. The FTIR spectrum of PVA (Figure 2C) showed that the peak shape at 3421 cm^{-1} attributed to the stretching vibration absorption peak of -NH2. The absorption peak moved towards higher 3608 cm^{-1} in the spectrum of La@PCDs, was attributed to the vibrational frequency of the chemical bonds during the process of electron absorption. The characteristic absorption peak at 1445 cm^{-1} and 1330 cm^{-1}as attributed to C=O stretching vibration. The peak shape was not changed when $La(NO_3)_3{\cdot}6H_2O$ reacted with PVA suggest that the generation of La@PCDs broke the carbon-oxygen bond to form novel chemical bond. To evaluate the prepared carbon dots, the fluorescence detection, quantum yield (QY)

and zeta potential were characterized (Figure 2E and F). According to the results, the material La@PCDs exhibits excellent fluorescence characteristics, as evidenced by the excitation and emission wavelengths depicted in the following figure Specifically, its excitation wavelength is 363nm (red line), while its emission wavelength at the optimal excitation wavelength is 490nm (black line). Notably, the Stokes Shift of La@PCDs was 127 nm indicating their advantageous features such as robust anti-interference capability, minimal light-induced damage to biological samples, remarkable penetration ability, and heightened detection sensitivity. The quantum yield (QY) of the La@PCDs was test based on a standard method which offers a value of 0.28% for the optimized La@PCDs in PBS buffer. The zeta potential is increased obviously from negative to positive value, which confirms an opposite charge surface and suggests a possible electrostatic force driving the assembly of La@PCDs.

pH-Dependent in vitro ROS Release

Numerous studies have demonstrated that the eradication or substantial reduction of biofilm by producing ROS is a promising antibacterial strategy.[23,24] ROS are a group of chemical compounds generated during the incomplete reduction process of oxygen, and include singlet oxygen ($^1O_2$), superoxide anions ($O_{2\cdot-}$), hydrogen peroxide (H_2O_2) and hydroxyl radicals (OH). These compounds possess potent antimicrobial properties and can effectively eradicate microorganisms without increasing the risk of resistance.[25] In this study, we evaluated the catalytic efficiency of La@PCDs for ROS generation. To quantify the total ROS production, DCFH-DA was used as an indicator. Upon exposure to ROS, DCFH-DA is oxidized, resulting in the formation of 2.7-dichlorofluorescein (DCF), which exhibits intense luminescence at 525 nm (I_{525}).[26] The absorption spectrum of the QCD-PVA at 525 nm (I_{525}) showed minimal changes in the absence of La. However, the presence of La@PCDs significantly enhanced the absorption of I_{525} over time (Figure 3A), indicating that La plays a vital role in the generation of

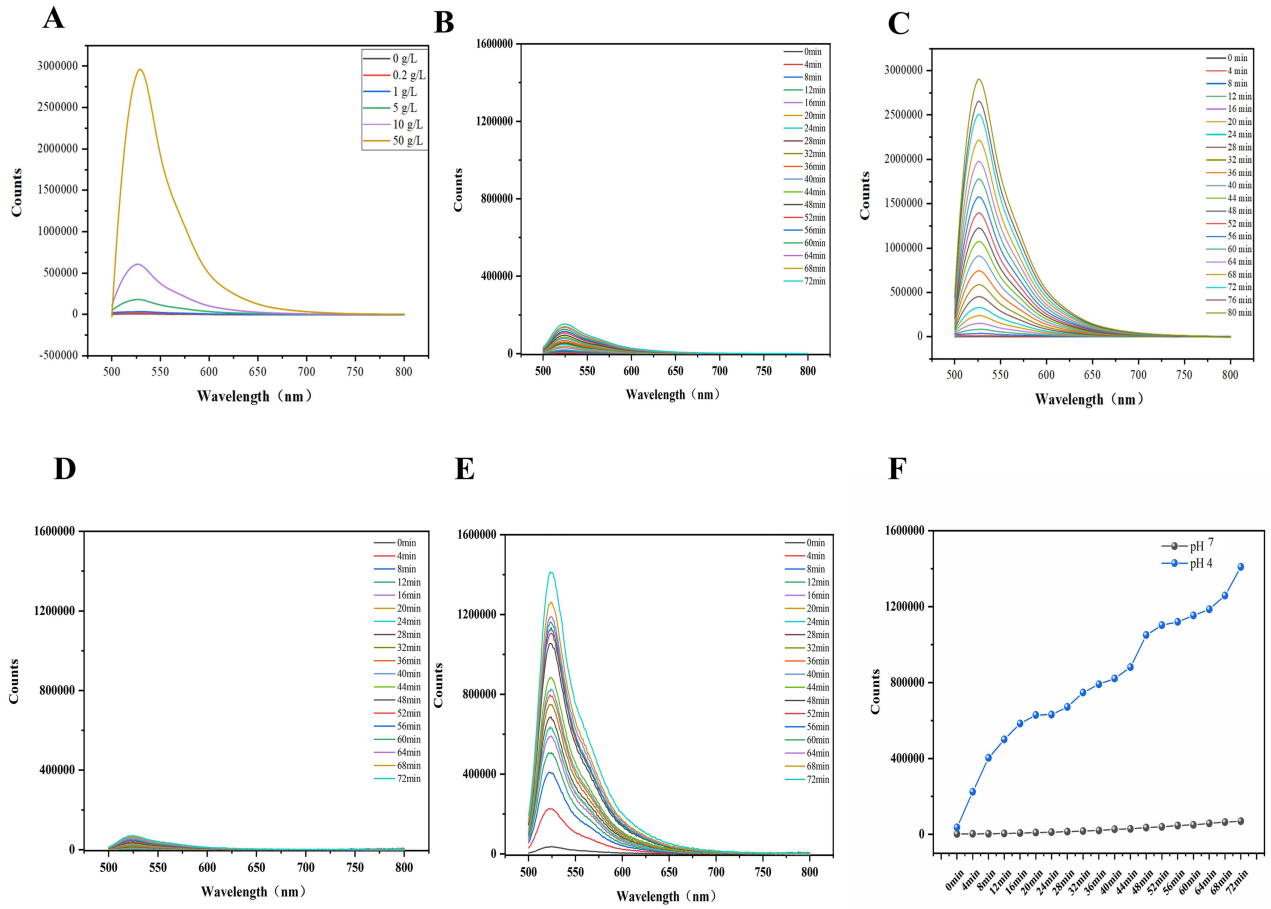

Figure 3 UV−vis absorption spectra of DCFH-DA in different solutions: (**A**) different concentrations of lanthanum in La@PCDs (**B**) LaNPs (**C**) La@PCDs (**D**) La@PCDs at pH 7.0 (**E**) La@PCDs at pH 4.0 (**F**) Typical absorbance changes of different pH.

ROS. In addition, the catalytic rate strongly depends on the La concentration in the La@PCD composite materials (Figure 3A), demonstrating that it is a dose-dependent functional nanomaterial. Electron holes in the La 4f orbital can react with air and water in the surrounding environment, resulting in the generation of a limited quantity of ROS.[27] The fluorescence signal at 525 nm wavelength in the LaNPs group increased slightly. The introduction of CQD-PVA promoted the ROS generation of because CQD-PVA facilitates the oxidative activity of La. As anticipated, after modification with CQD-PVA, the La@PCDs displayed much stronger fluorescence intensity (Figure 3B and C). This may be because the abundant positive charge of CQD-PVA on the surface is coupled with electron holes in the La 4f orbital, increasing the generation of ROS.

It is noteworthy that the catalytic efficiency of the La@PCDs was influenced by different pH levels. The fluorescence of I_{525} was minimal at PH 7.0, but a significant increase in fluorescence intensity at I_{525} is observed at pH 4.0 (Figure 3D and E), indicating the responsiveness of DCF to ROS under acidic conditions. Therefore, a PBS buffer (pH 4.0) was selected because of its effectiveness in detecting the ROS production facilitated by La@PCDs. These results demonstrate that the La@PCDs behave as a type of biomaterial for pH-responsive nanoagents (Figure 3F). The acidic environment inside the biofilm lays the foundation for future antibacterial applications. The acidic microenvironment in biofilms is caused by the build-up of acid metabolites produced through anaerobic fermentation by embedded microbes.[28] These hypoxic and acidic conditions boost microbial tolerance to conventional antibiotics within the biofilm, resulting in chronic infection.[29] Generally, bacteria residing in biofilms demonstrate antibiotic resistance levels approximately 1000 times greater than those observed in planktonic bacteria.[30] Although the challenges posed by biofilm-associated infections render their eradication difficult, they present significant opportunities for the development of nanotherapeutic agents capable of responding to the unique microenvironments involved. The acidic conditions within biofilms require a design of therapeutic nanoagents which are responsive to acidity.[31] Recently, various pH-responsive platforms have been engineered to treat biofilm infections. These nanoparticles remain stable in normal physiological environments but undergo degradation or structural changes when exposed to acidic conditions, thereby facilitating drug release or activation.[32] As with the La@PCD nanoparticles synthesized in this study, under the stimulus of endogenous factors, the concentration of ROS in the biofilm undergoes a significant increase, resulting in enhanced efficacy for biofilm removal. Additionally, ROS accumulation in healthy tissues can be minimized, thereby mitigating potential adverse effects.

In vitro Antibacterial Activities

The minimal inhibitory concentration (MIC) and minimal bactericidal concentration (MBC) of LaNPs and La@PCDs were conducted through a modified technique involving microdilution in broth (Figures 4A and S2). According to the results, when the concentration of La@PCDs reached 0.5 mg/mL, it effectively suppressed the growth of E. faecalis to a low level, resulting in significant inhibition of proliferation. Hence, the minimum inhibitory concentration required for La@PCDs against E. faecalis was determined as 0.5 mg/mL. The MIC of LaNPs was determined as 8 mg/mL. The determination of MBC was conducted utilizing the agar plate dilution technique. The MBC of La@PCDs and LaNPs was determined as 0.5 and 16 mg/mL respectively.

E. faecalis, either alone or in combination with other microorganisms, has been identified as the primary causative agent of post-treatment infections with persistent periradicular lesions, with frequencies ranging from 24% to 77%.[33,34] The ability of E. faecalis to survive in a post-endodontic environment can ascribe its unique capacity to modulate host responses, suppress lymphocyte activity, sustain prolonged periods of nutrient deprivation, utilize serum as a source of nourishment, and exhibit genetic variability.[35] Moreover, E. faecalis demonstrates strong dentin adhesion properties and penetration into dentinal tubules, while also forming biofilms that are resistant to conventional antimicrobial agents commonly used during initial endodontic treatment.[36] Figure 4D and E show the optical density (OD) values obtained from different groups after incubating E. faecalis for 12 and 24 h, respectively, indicating their antibacterial performance. The H_2O group did not exhibit any antibacterial effects as the OD values consistently remained high. The OD value of LaNPs group displayed a attractive increase after the 3rd dilution, but the La@PCD group displayed an increase after the 8th dilution, demonstrating that the antimicrobial activity of La was enhanced when combined with CQD-PVA. Interestingly, a "hormesis effect" was observed in the LaNPs group, in which the OD value exceeded the high level of the H_2O group after 5th dilution. The literature indicates that La exhibits a "hormesis effect" in antibacterial activities due to its inherent instability.[37] Our experimental findings also validate this phenomenon, whereas the combination with CQD-PVA eliminates it, thereby suggesting the role of CQD-PVA in stabilizing La. The control group containing 5% NaClO demonstrated an increase in the OD value after the 6th dilution. Based

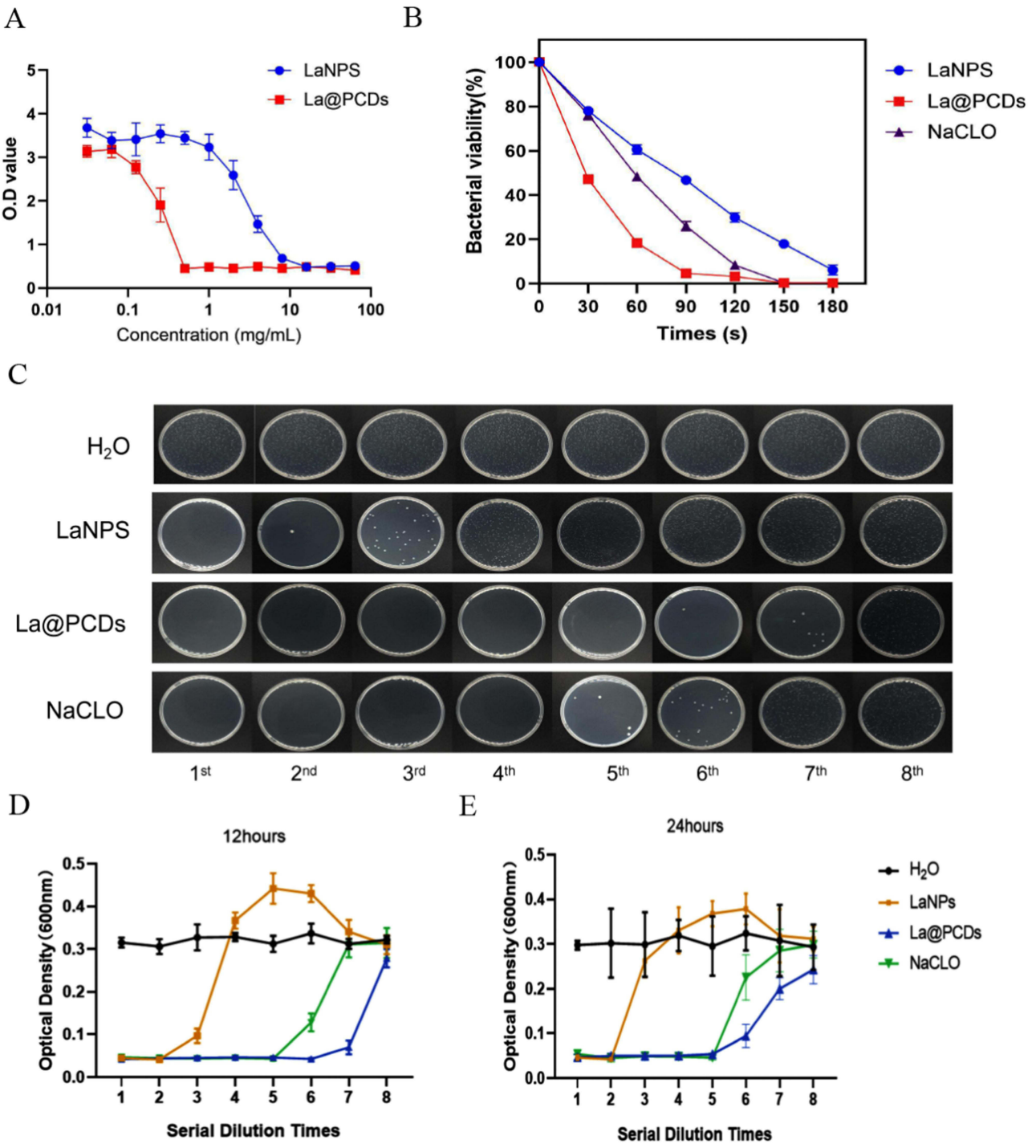

Figure 4 (**A**) Minimum inhibitory concentration curve of LaNPs and La@PCDs to E. faecalis (**B**) kinetic curve of bacterial inhibition of LaNPs, NaCLO and La@PCDs during the 3 minutes. (**C**) A coated flat panel was utilized to evaluate the effects of different materials on E. faecalis. E. faecalis samples treated with various reagents at different dilutions following incubation periods of (**D**) 12 hours and (**E**) 24 hours.

on these findings, it can be inferred that the La@PCDs possess antibacterial properties comparable to those of the 5% NaClO solution. Relevant findings from the plate counting results also supported the comparable effectiveness of the antibacterial properties (Figure 4C). The results of silver complexes the kinetic curve of bacterial inhibition as shown in Figure 4B. E. faecalis show a remarkably rapid response in the presence of La@PCDs.

Anti-Biofilm Activities in vitro

Biofilms play a pivotal role in various chronic bacterial infections. Microorganisms are encapsulated within extracellular polymeric substances (EPS) that provide a protective shield against body's defense systems and enhance resistance to numerous biocides or antibiotics. Typically, the antibiotic resistance of bacteria residing in biofilms is 1000 times higher than planktonic bacteria.[23,24] However, ROS can attenuate and degrade the matrix structure and EPS by targeting multiple biomolecules. Several nanomaterials have been developed for cancer treatment and antimicrobial therapy by harnessing their ability to generate ROS. Excessive generation of ROS has the potential to overwhelm the antioxidant defense mechanisms employed by microbial cells.[38] Upon production, ROS selectively targets various molecules in close proximity, including polysaccharides within the biofilm matrix, lipids on cell surfaces, proteins, and intracellular DNA. This ultimately leads to the degradation of the biofilm matrix and disintegration of microbial cells.[39] In this study, the combination of La and CQD-PVA has been shown to generate a significant amount of ROS, making La@PCDs an efficient alternative approach.

Fluorescence microscopy was used to validate the efficacy of the nanoplatform in eradicating E. faecalis biofilms. In Figure 5A, representative images demonstrate that live bacteria are stained green, whereas dead bacteria are stained red. In the control group, the plate was predominantly covered with vigorously proliferating green-stained live bacteria.[39] The anti-biofilm activities of La were negligible compared with those of the control group. However, red bacteria were observed in the LaNP group, suggesting improved antimicrobial activity compared with the control group. In contrast, treatment with the La@PCDs effectively eradicated most of the biofilms, resulting in minimal viable bacteria. As predicted, the ROS generated by combined treatment with lanthanum and CQD-PVA successfully removed the biofilm. Although NaClO exhibited strong antimicrobial effects, its ability to remove biofilm was not as potent as that of La@PCDs.

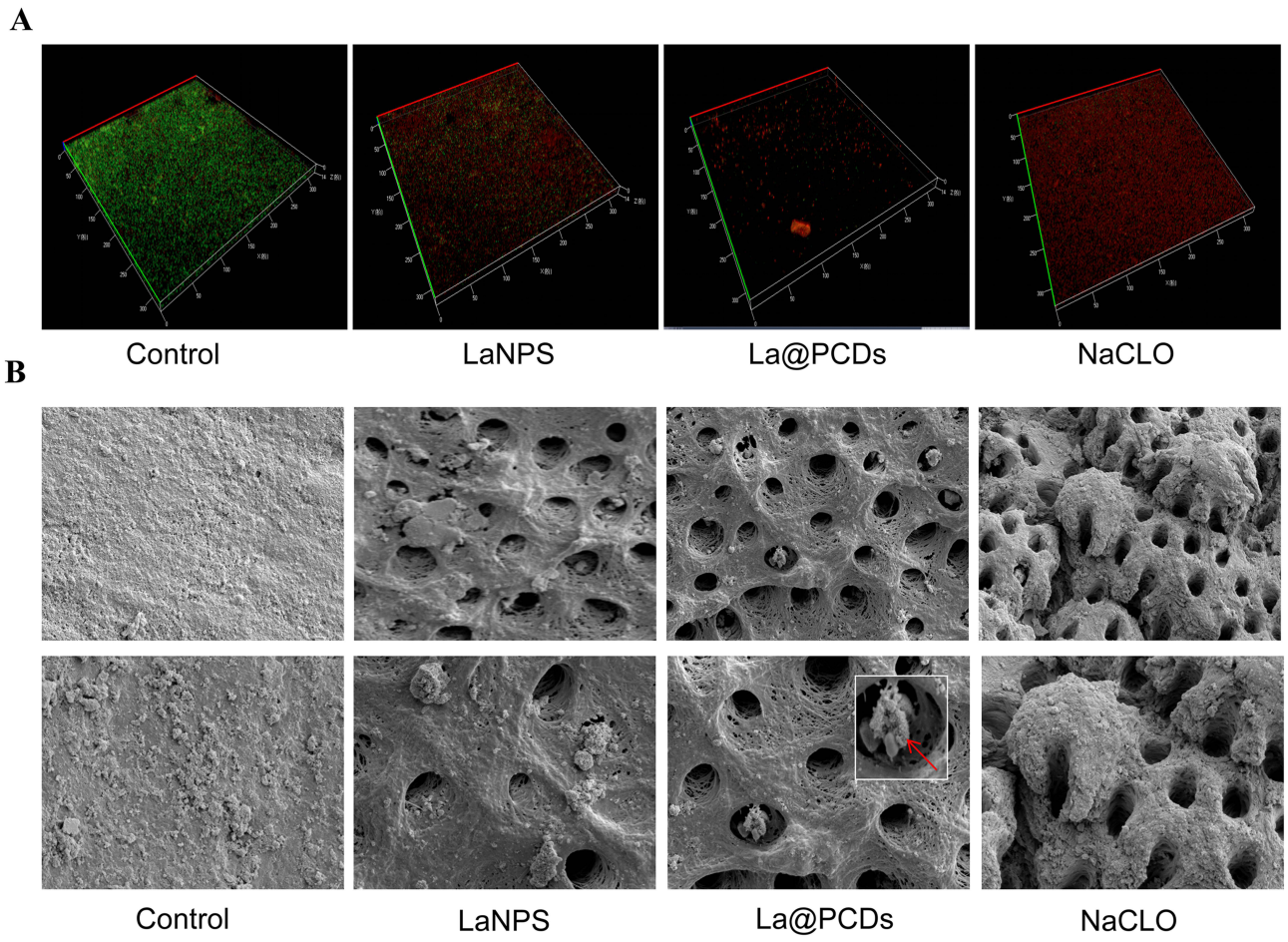

Figure 5 (**A**) CLSM images of E. faecalis biofilms after different treatments (**B**) SEM images of E. faecalis biofilms eradication after different treatments in a dentin root canal wall. (The inset boxes in the panel reveal E. faecalis became flattened and damaged after irrigation of La@PCDs).

In situ Biofilm Removal in Root Canal System

A simulated root canal model was used to investigate the efficacy of various irrigants in eradicating biofilms and infected dentinal tubules within the root canal. The establishment of the E. faecalis biofilm within the root canal system followed the study completed by Ye's study.[22] After four weeks of incubation, the biofilm was treated with different agents. SEM images of the control group treated with water revealed dense colonization of E. faecalis on the walls of the root canal, effectively obstructing the dentinal tubules (Figure 5B). These findings implied the successful formation of E. faecalis biofilms within the root canal system. Similar results were observed in the LaNP group, demonstrating a weak removal of biofilm accumulation following treatment with LaNPs. However, most of the biofilm was effectively eradicated in the La@PCD group, exposing the dentin tubules. Nanoparticles were attached around the openings of the dentin tubules, leading to deformation and flattening of any remaining E. faecalis bacteria, indicating their complete elimination (Figure 5B). Although the NaClO groups exhibited a low level of bacterial colonization, treatment with NaOCl resulted in noticeable erosive alterations in the root canal dentin, while no apparent damage was observed in the other groups (Figure 5). Previous studies demonstrated that NaOCl possesses exceptional tissue-dissolving capabilities and can effectively dissolve necrotic tissue and organic compounds present in smear layers.[8] Umer et al revealed that dentin surfaces treated with NaOCl exhibited reduced collagen content and nonuniform deproteinization channels, resulting in brittle dentin.[2] This effect may create inconspicuous pathways for bacteria, particularly E. faecalis, to penetrate and spread through these spaces, ultimately leading to microleakage, which is a prominent cause of root canal failure.[2] In summary, La@PCDs demonstrated bactericidal and anti-biofilm properties comparable to those of commercially available NaClO solutions without causing significant damage to the structure of dentin.

Cytotoxicity Assessment

The cumulative effects of these agents on L929 cell viability are shown in Figure 6. The results of the CCK-8 assay indicated that NaClO exhibited significant cytotoxicity towards the cells, as evidenced by their near-zero viability. Conversely, the other two groups demonstrated cell viability comparable to that of the control group (Figure 6A). This observation was reinforced by fluorescence microscopy of the stained cells (Figure 6B). The cells exposed to La@PCDs and LaNPs appeared healthy and exhibited an intact morphology with red-fluorescent cytoplasm and blue-fluorescent nuclei. The distribution and morphology of cells in these two groups were indistinguishable from those in the control

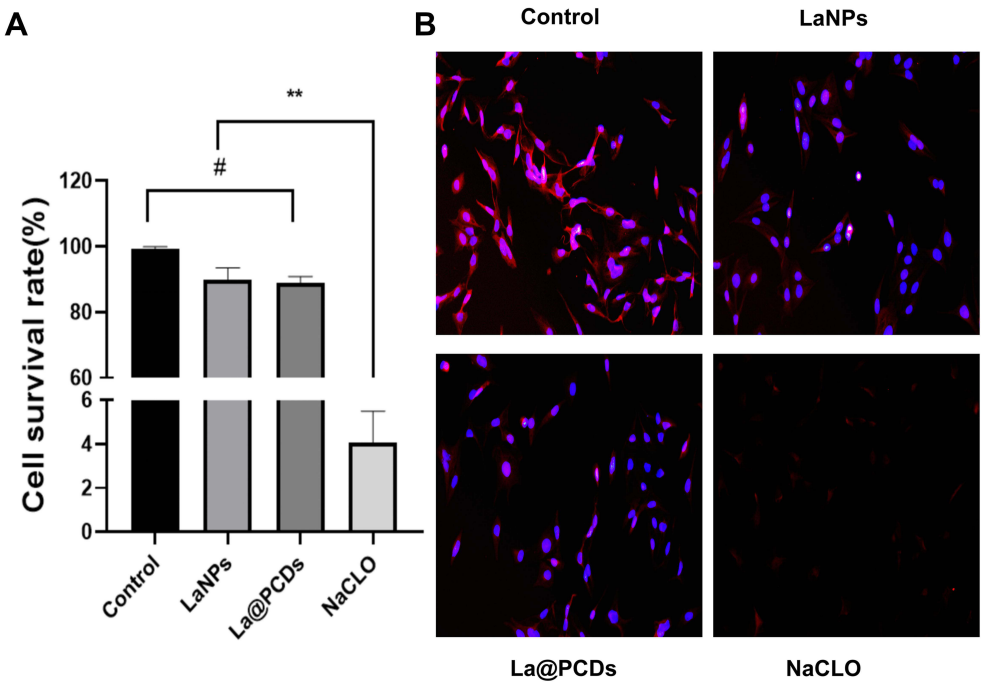

Figure 6 Cytotoxicity assessment of different reagents. (**A**) Cell viability of L929 cells (n=3). **p < 0.01, #p>0.05. (**B**) Morphology of L929 after different treatments.

group. As expected, NaClO demonstrated pronounced cytotoxicity, resulting in an almost complete absence of viable cells after exposure. These findings underscore the successful integration of our nanoparticles, wherein the combination of rare earth elements with CQD-PVA facilitates the rapid generation of ROS. The transient lifespan of the ROS enabled the nanoparticles to exhibit remarkably efficient bactericidal properties without inducing residual cytotoxic effects.

In recent years, there have been widespread applications of nanomaterials capable of generating ROS for cancer treatment and combating microbial infections.[26] However, it is important to note that while elevated levels of ROS can be utilized to induce cell death for therapeutic purposes, excessive ROS production after fulfilling its intended function may lead to oxidative damage to surrounding healthy tissues.[40] Therefore, striking a balance between the therapeutic benefits and the potential side effects of ROS has become crucial for optimizing the effectiveness of ROS-associated nanomedicines. One effective approach to achieve this goal is to implement stimuli-responsive strategies that allow for maximum therapeutic effects during disease treatment while minimizing harm to normal tissues. As mentioned previously, La@PCDs are nanoparticles that specifically respond to changes in pH and trigger ROS generation only under acidic conditions. This implies that La@PCDs remain stable within the normal physiological environment of the body but become activated when exposed to an acidic biofilm microenvironment caused by anaerobic fermentation by microbes. From a safety standpoint, this activation process ensures that only limited amounts of ROS are generated, and any potential damage caused by these short-lived molecules can be disregarded without acid activation.

Conclusion

This study innovatively synthesized a novel nanofunctional material, La@PCDs, by combining CQD-PVA and lanthanum for root canal irrigation. The synergistic effect of CQD-PVA and La resulted in a high bactericidal efficacy through ROS generation. This approach demonstrated superior efficiency in antibacterial under acidic conditions without causing significant cytotoxicity compared to the commonly used NaClO irrigant. Although well-pleasing antimicrobial effect and biosafety were confirmed, further investigations are required to clarify its antibacterial mechanisms and effectiveness against diverse bacterial strains, and to optimize its usage before translating these preclinical findings into dental medical advancements. Overall, these results suggest that La@PCDs represent a promising strategy for eradicating biofilms, with significant potential for treating endodontic infections.

Acknowledgments

This work was financially supported by North Rare Earth Group Technology Project ”Functional Application of Lanthanum Cerium Oxide in Cooling Fabric, High Temperature Ink Heat Dissipation, and Oral Antibacterial Effects” (Project Number: BFXT-2023-D-0004), Tianjin Stomatological Hospital Key Medical Discipline Project (2022EK01)

Disclosure

The authors report no conflicts of interest in this work.

References

1. Sun D, Pang X, Cheng Y, et al. Ultrasound-switchable nanozyme augments sonodynamic therapy against multidrug-resistant bacterial infection. *ACS Nano*. 2020;14(2):2063–2076. doi:10.1021/acsnano.9b08667
2. Daood U, Bapat RA, Sidhu P, et al. Antibacterial and antibiofilm efficacy of k21-E in root canal disinfection. *Dent Mater*. 2021;37(10):1511–1528. doi:10.1016/j.dental.2021.08.001
3. Berlanga M, Guerrero R. Living together in biofilms: the microbial cell factory and its biotechnological implications. *Microb Cell Fact*. 2016;15(1):165. doi:10.1186/s12934-016-0569-5
4. Boutsioukis C, Arias-Moliz MT. Present status and future directions - irrigants and irrigation methods. *Int Endod J*. 2022;55(Suppl 3):588–612. doi:10.1111/iej.13739
5. Keogh D, Tay WH, Ho YY, et al. Enterococcal metabolite cues facilitate interspecies niche modulation and polymicrobial infection. *Cell Host Microbe*. 2016;20(4):493–503. doi:10.1016/j.chom.2016.09.004
6. Deng Z, Lin B, Liu F, Zhao W. Role of Enterococcus faecalis in refractory apical periodontitis: from pathogenicity to host cell response. *J Oral Microbiol*. 2023;15(1):2184924. doi:10.1080/20002297.2023.2184924
7. Heidar SA-HA, Saber SE, SA-LA-A E, El-Ashry SH. Antibacterial potential of nano-particulate intracanal medications on a mature E. faecalis biofilm in an ex-vivo model. *Giornale Italiano di Endodonzia*. 2020;34(2):1.
8. Tartari T, Bachmann L, Maliza AG, Andrade FB, Duarte MA, Bramante CM. Tissue dissolution and modifications in dentin composition by different sodium hypochlorite concentrations. *J Appl Oral Sci*. 2016;24(3):291–298. doi:10.1590/1678-775720150524

9. Mendoza LJN, Montoya AC, Peñaloza TYM, Guerreroc CG. Biomechanical effect of irrigants in noninstrumented dentin: systematic review and meta-analysis. *Crit Rev Biomed Eng*. 2021;49(2):53–64. doi:10.1615/CritRevBiomedEng.2021038065
10. Elbahary S, Haj-Yahya S, Khawalid M, et al. Effects of different irrigation protocols on dentin surfaces as revealed through quantitative 3D surface texture analysis. *Sci Rep*. 2020;10(1):22073. doi:10.1038/s41598-020-79003-9
11. Jiang W, Xie Z, Huang S, et al. Targeting cariogenic pathogens and promoting competitiveness of commensal bacteria with a novel pH-responsive antimicrobial peptide. *J Oral Microbiol*. 2023;15(1):2159375. doi:10.1080/20002297.2022.2159375
12. Rodrigues CT, de Andrade FB, de Vasconcelos L, et al. Antibacterial properties of silver nanoparticles as a root canal irrigant against Enterococcus faecalis biofilm and infected dentinal tubules. *Int Endod J*. 2018;51(8):901–911. doi:10.1111/iej.12904
13. Chakka SV, Thanjavur N, Lee S, Kim S. Synthesis and characterization of lanthanum-doped curcumin-functionalized antimicrobial copper oxide nanoparticles. *J Rare Earths*. 2023;41(10):1606–1615. doi:10.1016/j.jre.2022.08.020
14. Hu C, Wang MX, Sun L, Yang JH, Zrínyi M, Chen YM. Dual-physical cross-linked tough and photoluminescent hydrogels with good biocompatibility and antibacterial activity. *Macromol Rapid Commun*. 2017;38(10). doi:10.1002/marc.201600788
15. Abdel Aziz AA, Sayed MA. Some novel rare earth metal ions complexes: synthesis, characterization, luminescence and biocidal efficiency. *Anal Biochem*. 2020;598:113645. doi:10.1016/j.ab.2020.113645
16. Ma T, Zhai X, Huang Y, et al. A smart nanoplatform with photothermal antibacterial capability and antioxidant activity for chronic wound healing. *Adv Healthc Mater*. 2021;10(13):e2100033. doi:10.1002/adhm.202100033
17. Yan B. *Photofunctional Rare Earth Hybrid Materials*. Vol. 251. Springer; 2017.
18. Kang Y, Li D, Dong R, et al. Multicolor carbon dots assembled polyvinyl alcohol with enhanced emission for white light-emitting diode. *J Lumin*. 2022;251:119164. doi:10.1016/j.jlumin.2022.119164
19. Abdullah ZW, Dong Y, Davies IJ, Barbhuiya S. PVA, PVA blends, and their nanocomposites for biodegradable packaging application. *Polym-Plast Technol Eng*. 2017;56(12):1307–1344. doi:10.1080/03602559.2016.1275684
20. Hoang Q-B, Mai V-T, Nguyen D-K, Truong D, Mai X-D. Crosslinking induced photoluminescence quenching in polyvinyl alcohol-carbon quantum dot composite. *Mater Today Chem*. 2019;12:166–172. doi:10.1016/j.mtchem.2019.01.003
21. Wang M, Su Y, Liu Y, et al. Antibacterial fluorescent nano-sized lanthanum-doped carbon quantum dot embedded polyvinyl alcohol for accelerated wound healing. *J Colloid Interface Sci*. 2022;608(Pt 1):973–983. doi:10.1016/j.jcis.2021.10.018
22. Ye WH, Yeghiasarian L, Cutler CW, et al. Comparison of the use of d-enantiomeric and l-enantiomeric antimicrobial peptides incorporated in a calcium-chelating irrigant against Enterococcus faecalis root canal wall biofilms. *J Dent*. 2019;91:103231. doi:10.1016/j.jdent.2019.103231
23. Hu X, Huang YY, Wang Y, Wang X, Hamblin MR. Antimicrobial photodynamic therapy to control clinically relevant biofilm infections. *Front Microbiol*. 2018;9:1299. doi:10.3389/fmicb.2018.01299
24. Gao F, Shao T, Yu Y, Xiong Y, Yang L. Surface-bound reactive oxygen species generating nanozymes for selective antibacterial action. *Nat Commun*. 2021;12(1):745. doi:10.1038/s41467-021-20965-3
25. Sies H, Jones DP. Reactive oxygen species (ROS) as pleiotropic physiological signalling agents. *Nat Rev Mol Cell Biol*. 2020;21(7):363–383. doi:10.1038/s41580-020-0230-3
26. Zhang CX, Li HW, Zhang R, Ren Z, Wu Y. Tumor microenvironments-adaptive apoptotic effects of cytidine 5'-monophosphate-capped gold nanoclusters. *ACS Appl Bio Mater*. 2022;5(7):3452–3460. doi:10.1021/acsabm.2c00380
27. Lukens WW, Speldrich M, Yang P, Duignan TJ, Autschbach J, Kögerler P. The roles of 4f- and 5f-orbitals in bonding: a magnetochemical, crystal field, density functional theory, and multi-reference wavefunction study. *Dalton Trans*. 2016;45(28):11508–11521. doi:10.1039/c6dt00634e
28. Hu Y, Ruan X, Lv X, et al. Biofilm microenvironment-responsive nanoparticles for the treatment of bacterial infection. *Nano Today*. 2022;46:101602. doi:10.1016/j.nantod.2022.101602
29. Pereira TC, Dijkstra RJB, Petridis X, et al. Chemical and mechanical influence of root canal irrigation on biofilm removal from lateral morphological features of simulated root canals, dentine discs and dentinal tubules. *Int Endod J*. 2021;54(1):112–129. doi:10.1111/iej.13399
30. Mohammadi Z, Jafarzadeh H, Shalavi S. Antimicrobial efficacy of chlorhexidine as a root canal irrigant: a literature review. *J Oral Sci*. 2014;56(2):99–103. doi:10.2334/josnusd.56.99
31. Wong J, Zou T, Lee AHC, Zhang C. The potential translational applications of nanoparticles in endodontics. *Int J Nanomed*. 2021;16:2087–2106. doi:10.2147/ijn.S293518
32. Nguyen AT, Goswami S, Ferracane J, Koley D. Real-time monitoring of the pH microenvironment at the interface of multispecies biofilm and dental composites. *Anal Chim Acta*. 2022;1201:339589. doi:10.1016/j.aca.2022.339589
33. Alghamdi F, Shakir M. The influence of enterococcus faecalis as a dental root canal pathogen on endodontic treatment: a systematic review. *Cureus*. 2020;12(3):e7257. doi:10.7759/cureus.7257
34. Jiao Y, Tay FR, Niu LN, Chen JH. Advancing antimicrobial strategies for managing oral biofilm infections. *Int J Oral Sci*. 2019;11(3):28. doi:10.1038/s41368-019-0062-1
35. Stuart CH, Schwartz SA, Beeson TJ, Owatz CB. Enterococcus faecalis: its role in root canal treatment failure and current concepts in retreatment. *J Endod*. 2006;32(2):93–98. doi:10.1016/j.joen.2005.10.049
36. Guneser MB, Eldeniz AU. The effect of gelatinase production of Enterococcus faecalis on adhesion to dentin after irrigation with various endodontic irrigants. *Acta Biomater Odontol Scand*. 2016;2(1):144–149. doi:10.1080/23337931.2016.1256212
37. Pagano G, Brouziotis AA, Lyons D, et al. Hormetic effects of cerium, lanthanum and their combination at sub-micromolar concentrations in sea urchin sperm. *Bull Environ Contam Toxicol*. 2023;110(3):65. doi:10.1007/s00128-023-03701-z
38. Juan CA, Pérez de la Lastra JM, Plou FJ, Pérez-Lebeña E. The chemistry of reactive oxygen species (ros) revisited: outlining their role in biological macromolecules (DNA, Lipids and Proteins) and induced pathologies. *Int J Mol Sci*. 2021;22(9):4642. doi:10.3390/ijms22094642
39. Guo J, Xu Y, Liu M, et al. An MSN-based synergistic nanoplatform for root canal biofilm eradication via Fenton-enhanced sonodynamic therapy. *J Mater Chem B*. 2021;9(37):7686–7697. doi:10.1039/d1tb01031j
40. Zhang C, Wang X, Du J, Gu Z, Zhao Y. Reactive oxygen species-regulating strategies based on nanomaterials for disease treatment. *Adv Sci*. 2021;8(3):2002797. doi:10.1002/advs.202002797